Nano Energy 69 (2020) 104419

Contents lists available at ScienceDirect

Nano Energy

journal homepage: http://www.elsevier.com/locate/nanoen

A universal and arbitrary tactile interactive system based on self-powered optical communication

Jinrong Huang [a,b], Xixi Yang [a,b], Jinran Yu [a,b], Jing Han [a,b], Chuankun Jia [c], Mei Ding [c], Jia Sun [d], Xiaole Cao [a,b], Qijun Sun [a,b,e,*], Zhong Lin Wang [a,b,f,**]

[a] Beijing Institute of Nanoenergy and Nanosystems, Chinese Academy of Sciences, Beijing, 100083, China
[b] School of Nanoscience and Technology, University of Chinese Academy of Sciences, Beijing, 100049, PR China
[c] College of Materials Science and Engineering, Changsha University of Science & Technology, Changsha, 410114, China
[d] School of Physics and Electronics, Central South University, Changsha, 410083, China
[e] Center on Nanoenergy Research, School of Physical Science and Technology, Guangxi University, Nanning, 530004, China
[f] School of Materials Science and Engineering, Georgia Institute of Technology, Atlanta, GA, 30332-0245, United States

ARTICLE INFO

Keywords:
Human-machine interaction
Self-powered optical communication
Triboelectric nanogenerators
Tactile interface
Universal system

ABSTRACT

Internet of Things (IoT) has diffused into practically every profession relying on various functional sensors and interactive interfaces. It is desirable to develop a cheap, facile, and energy-autonomous interactive system based on highly efficient optical communication. Here, we demonstrate a universal and stable tactile interactive system (TIS) on arbitrary objects through a self-powered optical communicator triggered by the triboelectric electric signals. The TIS includes a triboelectric nanogenerator (TENG) as the signal generator, a self-powered rectifying optical communicator, and a signal processing unit. Through the developed system, we can more effectively utilize the irregular/imperfect triboelectric signals to drive the optical communicator and implement various applications (including tactile switch, flowing LEDs, paper piano, PPT and domestic appliances wireless controller). The proposed TIS is simple in circuit design, capable of converting arbitrarily irregular/imperfect triboelectric signals and consumes low power and cost. It is believed the TIS will make great contributions to intelligent mechanosensation, precise digital control, smart home systems and advanced industrial manufacturing in future.

1. Introduction

Rapid development of electrical engineering, micro-electromechanical control and information technology has diffused Internet of Things (IoT) into practically every profession. Human-machine interactions relying on magnetic sensors [1,2], electrical transducers [3–6], mechanical controllers [7–10], and photodetectors [11,12] are the chief essentials to implement sensation, transduction, communication, and feedback. Even though numerous achievements have been made to popularize the interactive interfaces [13–15] by improving the sensitivity, flexibility and robustness [16–21], there are still great challenges on the wireless communication access, cost and power consumption reduction, and environmental noise alleviation [22–24]. Meanwhile, the cyber/digital security issues for authentication and identification in conventional HMI systems have become progressively worse due to the booming decoding and hacking techniques [25]. The maintenance-free and self-powered autonomous applications of HMI in the off-network circumstances are still lack of effective solutions depending on the distributed energy storage ways [26–28]. Scientists have been pursuing sustainable energy package or energy supply methods to long-term driving/maintaining the widely distributed sensors and interactive interfaces in the IoT. Different strategies have been developed by using triboelectric [29–33], photovoltaic [26,34], piezoelectric/piezoelectret [26,35–38], radiofrequency [35], and thermoelectric systems [35,39–42]. More direct and seamless combination of the interactive interfaces and autonomous energy supply is of great significance to achieve a universal and arbitrary communication system.

Among different interactive strategies, the optical communication is capable of fast and efficiently transmitting huge amount of information

* Corresponding author. Beijing Institute of Nanoenergy and Nanosystems, Chinese Academy of Sciences, Beijing, 100083, China.
** Corresponding author. Beijing Institute of Nanoenergy and Nanosystems, Chinese Academy of Sciences, Beijing, 100083, China.
E-mail addresses: sunqijun@binn.cas.cn (Q. Sun), zhong.wang@mse.gatech.edu (Z.L. Wang).

https://doi.org/10.1016/j.nanoen.2019.104419
Received 12 November 2019; Received in revised form 16 December 2019; Accepted 19 December 2019
Available online 26 December 2019
2211-2855/© 2019 Elsevier Ltd. All rights reserved.

and data in distant and radiation-free fashions [43–46]. It is applicable as either sensing components, transmission nodes, or intelligent application terminals in current IoT frameworks. In order to achieve effective and secure optical communication, it requires to use more specific optical transmission mediums or to develop complex encoding/decoding techniques [47,48]. This has limited the application of optical communication in the field of wireless control and decreased its transmission efficiency. Generally, the distributed optical communicator in IoT works in a full-time energy-consuming way for data transmission, even in the low-volume data exchange and the vacant period. This issue inevitably aggravates the energy dissipation and the preventive maintenance costs, which calls for more effective energy conservation technique. Based on triboelectrification and electrostatic induction, triboelectric nanogenerator (TENG) [49] has received widespread attention as micro/-nano power source to drive various sensors and controllers by converting mechanical energy into electrical energy. For example, fiber-based energy conversion devices have been widely used as candidates for effective conversion of biomechanical energy and self-powered interactive systems [37]. TENG hybridized with piezoelectrets is promising for self-powered acoustic transducers, flexible pressure sensors and wearable physiological monitors [38]. It is also capable of working as a self-powered active sensor or transducer for HMI system assisted with paired processing circuits to convert the pulse output signals into digital trigger signals [50–58]. The commonly used processing circuit in previous work includes an inductor, a capacitor, and a voltage comparator to deal with the intrinsic pulse signals [4,42,47,59], which is not an effective and universal circuit due to the required high threshold voltages and low resolution. Thus, it is highly desirable to develop a mechanical behavior derived interactive system by integrating TENG self-powered technique and optical communication.

In this work, we demonstrate a universal and stable tactile interactive system (TIS) on arbitrary objects through a self-powered optical communicator triggered by the triboelectric electric signals. The proposed TIS includes a TENG (arbitrary with any materials capable of triboelectrification) as the signal generator, an optical communicator (composed of a LED and a photoresistor), and a signal processing circuit. The signal collector can deliver the triboelectric signals (originated from the TENG induced by external actions, *e.g.* touch, press, contact, etc.) to driving the LED and photoresistor, through which the irregular/imperfect triboelectric signals can be rectified and work efficiently as the trigger signal for various functional terminals. The system has the following advantages: (i) the whole system is simple in the circuit design and consumes low power with commercial available materials and electronic components in low cost; (ii) the conventional output current level of TENG (~μA) can satisfy the power requirement and drive the optical communicator, which makes it facile to be designed on arbitrary objects on demand; (iii) it offers a universal way to converting the irregular/imperfect triboelectric outputs into effective trigger signals through the self-powered optical communicator. The proposed TIS will greatly expand the HMI systems to broader application scenes of intelligent control, pattern recognitions, smart robotics, and a variety of IoT related fields.

2. Results and discussion

HMI system is one of the basic interactive means in IoT [13,14]. Various sensors/transducer convert the external action (*e.g.* touch, slide, contact, wave, footstep, and even eye movement) into electrical signals, which are captured/read by the processing circuit and deliver relative orders to the functional terminals [4,5]. Compared with the conventional HMI system, the proposed TIS can utilize the TENG as the mechanosensor to convert external mechanical actions into electrical signals to drive the optical communicator in a self-powered way; then the mechanical actions give the specific orders to the processing circuit and drive the functional terminals (*e.g.* domestic appliance, entertainment/educational facilities and digital office equipment, Fig. 1a). Generally, any two different materials capable of triboelectrification can be utilized to fabricate the TENG mechanosensor, which is beneficial for the broad range of materials selection [56]. In different circumstances, people can take use of the proper materials originated from themselves to construct the TENG for convenient purposes and in low cost. For example, paper based TENG mechanosensor for TIS on papers are cheap, tailorable, folded and easy to design; using cloth or textile for the wearable TIS has the advantages of softness, breathability and easy cleaning. Furthermore, the TENG mechanosensor not only offers a self-powered driving fashion with broad choice of active materials, the multiple basic working modes (contact-separation, sliding, single electrode and free-standing) [56] greatly expand the application scenes and improve the versatility of the interactive system. It can be designed in the common thin-film structure and constructed on the paper/-plastic/textile substrates. It is also free of various shape designs following either one of the four basic working modes, *e.g.* a triboelectric tactile switch based on the transparent graphene electrodes or a ring-shaped controller based on flexible polymer materials (Fig. 1b). The facile and arbitrary design of the TENG mechanosensation components is promising for the bright prospects of the proposed TIS due to the broad choice of materials and multiple alternative working modes. The next issue is how to effectively capture/read the triboelectric signals.

Schematic illustration of the TENG in contact-separation mode is shown in Fig. 2a. The commonly utilized friction materials are copper (Cu) and fluorinated ethylene propylene (FEP) due to the enough electronegativity difference [56]. The basic working mechanism can be described by the coupling of contact electrification and electrostatic induction. Under the external force, Cu and FEP will have physical contact. According to the triboelectric series, electrons transfer from copper to FEP, producing a net positive charge on the copper surface and a net negative charge on the FEP surface, respectively. Once the two materials are separated, an electric potential difference is established between the two electrodes. In order to neutralize the potential difference between the two electrodes, the electrons are transferred from one electrode to another through an external circuit. Fig. 2b represents the typical electrical outputs of TENG including the short circuit current (I_{SC}) and open circuit voltage (V_{OC}) measured by the electrometer (Keithley 6514). The peak values of I_{SC} and V_{OC} of the TENG with an effective contact area of 5 × 5 cm^2 are 25 μA and 280 V, respectively. Both the I_{SC} and V_{OC} are consistent with typical output characteristics of TENG (*i.e.* relatively high output voltage and low current in pulse-shaped signals), which generally needs complex post-processing circuit (at least three components: a notch filter, an instrumentation amplifier and a single-chip microcomputer based latching relay) for the practical applications [19]. The conventional processing circuit is suitable for dealing with the standard clear and clean pulse output signals. However, if we zoom in the output pluses in Fig. 2b, the enlarged single pulse is actually an irregular pulse signal (Fig. 2c), which commonly exists in the output characteristics of the TENG when the two friction layers have imperfect contact-separation states. As shown in the left coordinates of Fig. 2c, it is supposed that only one pulse exists according to one cycle of the contact-separation process. However, a second smaller pulse followed with a tail wave shows up and disturbs the intrinsic single pulse characteristic. The phenomenon similar with the signals from damped vibration may be attributed to the vibrations of the friction layers or the supporting substrate after one cycle of contact-separation (Fig. 2d(ii) and Video S1). For the irregular output voltage pulse (right coordinates in Fig. 2c), it exhibits three peaks in the positive pulse direction, which may be attributed to the high surface roughness (Fig. 2d(iii)) or the height deformation (Fig. 2d(iv)) of the friction layers results in the unconformal and stepped contact between two friction layers. To verify this assumption, we have characterized the surface roughness of three types of commonly used friction materials (FEP, Cu electrode and polytetrafluoroethylene (PTFE)) by using profilometer (Dektak XT). As shown in Fig. S1, the surface profiles of the tested friction materials are all at ~μm level. For the copper foil

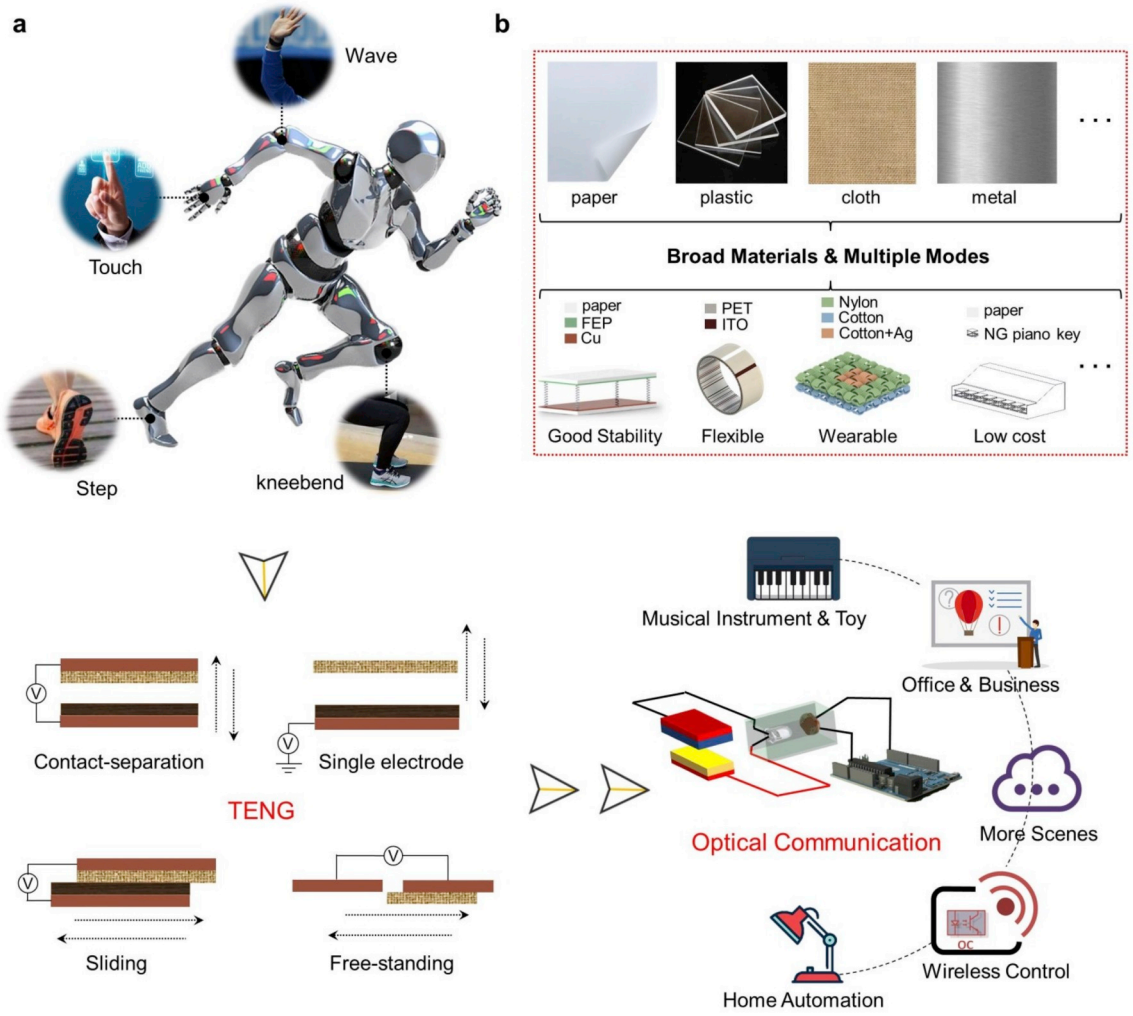

Fig. 1. The overview of the tactile interactive interface based on self-powered OC. (a) The concept of the TIS. The movement of human body can produce a variety of mechanical stimuli, which can be detected by different modes of TENG. The triboelectric signals can be converted as the trigger signals to functional terminals. (b) Broad optional materials (any materials are capable of contact electrification) and multiple modes of TENG mechanosensor.

electrode, the amplitude between peaks and troughs even reaches ~10 μm. This is a strong proof for the assumption of imperfect contact-separation (Fig. 2d(iii)). The irregular output signals are not limited to the above discussed situations, some of which cannot be precisely recognized by the previously reported processing circuits. Hence, a facile, effective and universal processing unit is highly desired to handle arbitrary output signals of TENG.

Supplementary video related to this article can be found at https://doi.org/10.1016/j.nanoen.2019.104419.

Fig. 3a shows the schematic illustration of the proposed TIS, which comprises of TENG mechanosensation component, self-powered optical communicator (OC), and microcontroller unit (MCU). The TENG works as the mechanosensor to collect the external action order from tactile, touch, sliding, pressing, hand waving, arm/leg bending, or stepping, and converts it into electric signal. Then, the sensing pulse signal (regular or irregular) is used to drive a LED and modulate the resistance of a photoresistor, constituting a self-powered optical communicator. Meanwhile, the threshold trigger voltage ($V_{trigger}$) in TIS is modulated through a bleeder circuit, which can be effectively recognized by the microcontroller and the embedded software program. The corresponding circuit diagram of TIS is shown in the bottom panel of Fig. 3a. The sensing electrical signal detected by the TENG mechanosensor drives the LED to modulate the resistance of the photoresistor in the follow-up bleeder circuit. In part (i) and (ii) of the TIS, the original TENG sensing signal is used to drive a LED. Then the optical signal of LED driven by TENG sensor (related with external actions) can be sensitively captured by the integrated photoresistor. This is the operation process of the OC system (part (ii)), which plays an important role in eliminating the imperfect or ineffective trigger effect originated from the irregular signals from TENG. As long as the irregular TENG signals can light up the paired LED (drive voltage > 2.2 V; drive current > 2 μA, which are easily achieved by the TENG), they can be converted into optical signals to modulate the resistance of the photoresistor and switch it on to supply a clean threshold signal through the bleeder circuit. Thus, the threshold signal will be delivered to the following part (iii) of TIS. Part (iii) (*i.e.* MCU) not only supplies the power for the bleeder circuit to achieve stable $V_{trigger}$ output related with the external action. It can also recognize $V_{trigger}$ and deliver the information to the embedded software program to realize various terminal functions (Fig. S2). Compared with previously reported processing circuit, the TIS is free of notch filter and instrumentation amplifier by taking advantage of the sophisticated combination of MCU and embedded programs, which greatly simplifies the signal processing circuit.

Interesting, the working process of the self-powered OC is similar with a transistor or a logic gate, *i.e.*, the LED light can be considered as the "gate" to modulate the current in the bleeder circuit of two resistors (the variable photoresistor and the paired load resistor) connected in series (Fig. 3b). The photoresistor resistance (R_{photo}) is variable

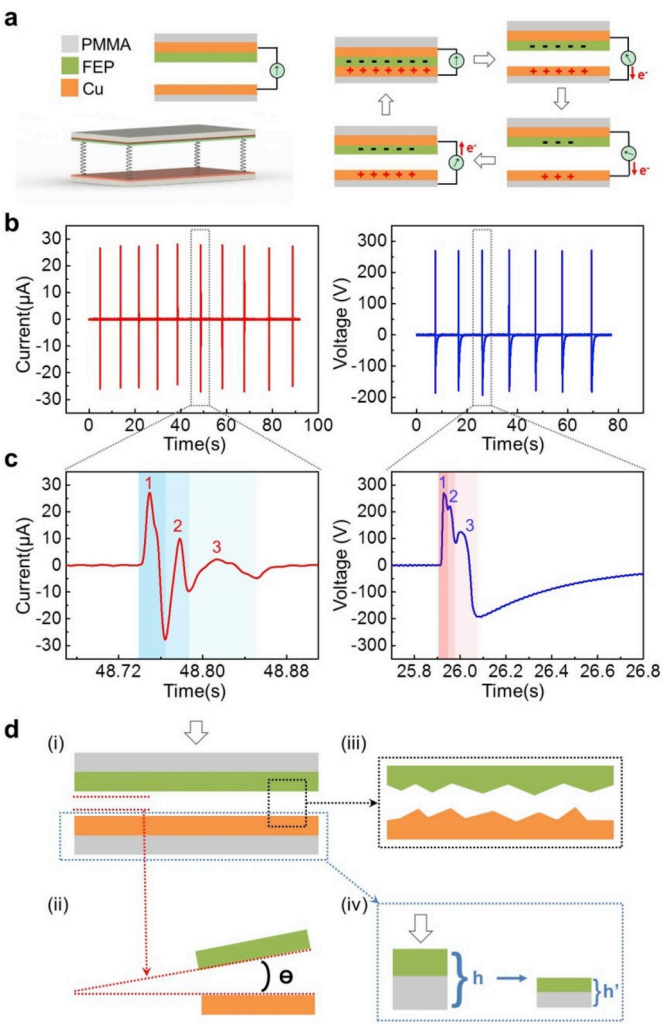

Fig. 2. (a) Schematic illustration of the TENG in contact-separation mode. (b) Typical electrical outputs of TENG including the short circuit current and open circuit voltage. (c) The enlarged irregular pulse signals produced by TENG. (d) Possible circumstances of the imperfect contact-separation process.

according to the LED light, while the resistance of the load resistor (R_{load}) is paired at ~10 KΩ. When there is no external action to drive LED through TENG mechanosensor, R_{photo} is high and the current flows through the R_{photo} is low. As the current is same for R_{photo} and R_{load} in the series circuit, the output voltage (V_{out}) is pulled up to 3.3 V. In contrast, when the external action is applied to the TENG mechanosensor, the photoresistor can detect the LED light and R_{photo} is decreased. The current flowing through the R_{photo} increases and leads to the pulling down of V_{out}. The high/low level of V_{out} can be recognized by the MCU as the $V_{trigger}$ for functional terminals. Both the photoresistor and the load resistor are commercial available, which is critical for the robust durability of TIS and greatly reduce the cost. To achieve fast response of the TIS, we select several typical photoresistors in different models (5539, 5549, 5528, 5516, 5506, 5537, and 12528, **Supplementary Note**) and investigate the voltage transfer characteristics (Fig. 3c). When the input voltage (V_{in}) increases from 0 to 4 V, all the V_{out}s decrease from 3.3 to ~0 V. Thereinto, the bleeder circuit with R_{photo} of 5516 model (green curve in Fig. 3c) takes the shortest response time to decrease to 0.3 V at V_{in} = 2.2 V. Real-time tests are also conducted to verify the stability of the TIS. A cycle sine wave (0–4 V, Fig. 3d) is input to the OC, stable square wave (0–3.3 V) is observed as shown in Fig. 3e. The above results demonstrate the TIS can successfully achieve the analog to digital conversion in a fast and stable way.

Fig. 4 shows the corresponding applications based on the proposed TIS on different substrates. The first demonstration is a graphene touch switch based on single-electrode mode TENG, composed of transparent graphene electrode and polyethylene terephthalate (PET) touch layer [60]. Schematic illustration is shown in Fig. 4a. When we touch the graphene mechano-switch (1, 2 or 3), the triboelectric signals induced by the electrostatic induction between the finger and PET can be recognized by the TIS and used to turn on/off the LEDs and color fans in the custom minute city views (Video S2). The TIS in this application, working as a touch switch based on the mechanism of tribo-electrification and electrostatic induction, offers an alternating interactive way to IoT and smart city, which is transparent, self-powered and facile to fabricate. Next, the TIS based on the contact-separation mode TENG mechanosensor is demonstrated to control the programmed flowing LEDs (Fig. 4b, Figs. S3 and S4). The mechanosensor is made of Cu/FEP/Cu on paper substrate. The electrostatic charges originated from contact electrification induce an output voltage to drive the OC, which pulls down the $V_{trigger}$. The pulling down of $V_{trigger}$ is subsequently monitored by the MCU and triggers the embedded programs for flowing LEDs. When the left Cu/FEP is contacted, the red LEDs light up one by one from the right side to the left side. When the right Cu/FEP is contacted, the green LEDs light up in the same direction. Dynamic controls on the flowing LEDs are exhibited in the Video S3. We further demonstrate a more complex paper piano (including both audios and videos) based on the TIS with the same mechanosensor design (Cu/FEP/Cu). Schematic illustration and photo image of the paper piano are shown in Fig. 4c, which includes eight basic notes from "do-re-mi-fa-so-la-ti" to higher-note "do". Each of the piano key is a TENG mechanosensor related to the channel 1 to 8, the signals of which can be recognized separately. It is observed that the originally irregular and messy current signals are converted into the standard digital signals through the self-powered OC that can be directly read by the MCU (Fig. 4d). Once we touch on either of the keys to make an effective contact-separation action, corresponding triboelectric signals can be captured and trigger the embedded audio/video programs simultaneously. Based on this system, various instruments can be achieved by simply re-burning the corresponding codes into the MCU. Videos S4 and S5 show the graceful and smooth melody played by the TIS based paper piano. Notably, according to the intrinsic pulse characteristic of TENG outputs, the signals are generated only at the moments of contact and separation, which leads to the instantaneous piano note. In order to realize piano notes following the human action (*e.g.*, touch or pressing), we integrate a resistive sensor with the TENG sensor, which can be used to recognize both the continuous and instantaneous actions, respectively. Video S6 shows the continuous piano notes under finger pressing. The above results demonstrate the excellent performance of the proposed TIS based on the self-powered optical communication, which also implies the broad prospects of the TIS in IoT, intelligent control and pattern recognition.

Supplementary video related to this article can be found at https://doi.org/10.1016/j.nanoen.2019.104419.

To satisfy the application requirements for wearable remote control system in more scenes, a wireless Bluetooth component can be integrated to expand the TIS with more sophisticated functions. Fig. 5a shows the concept of the wearable TIS (built in clothes or mounted on the ring) for wireless control applications (*e.g.* office software, domestic appliance, or entertainment/education facilities). The wireless TIS consists of two parts: the transmitting terminal and receiving terminal. The basic working process is shown in Fig. 5b. The transmitting terminal includes the TENG mechanosensor for generating the trigger signal, the self-powered OC for converting the trigger signal into a digital signal, the MCU for processing the digital signal, and a Bluetooth (or infrared) transmitter for wirelessly transmitting the trigger signal. The Bluetooth (or infrared) receiver at the receiving terminal captures the trigger signal sent by the transmitter through the corresponding protocols and translates the program instruction to control the target functional terminals.

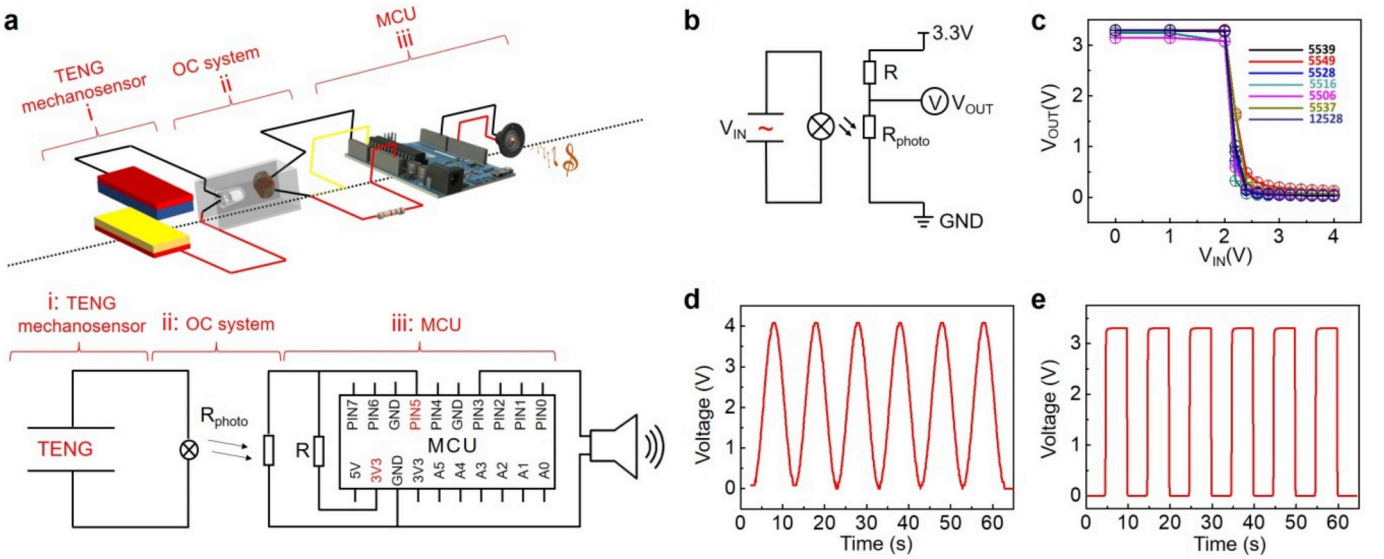

Fig. 3. (a) Schematic illustration and circuit diagram of the proposed TIS. (b) Circuit diagram of the self-powered OC and corresponding bleeder circuit. (c) Voltage transfer characteristics of the self-powered OC. (d) The input voltage to OC in sine wave form. (e) The achieved stable output in square wave form after bleeder circuit processing.

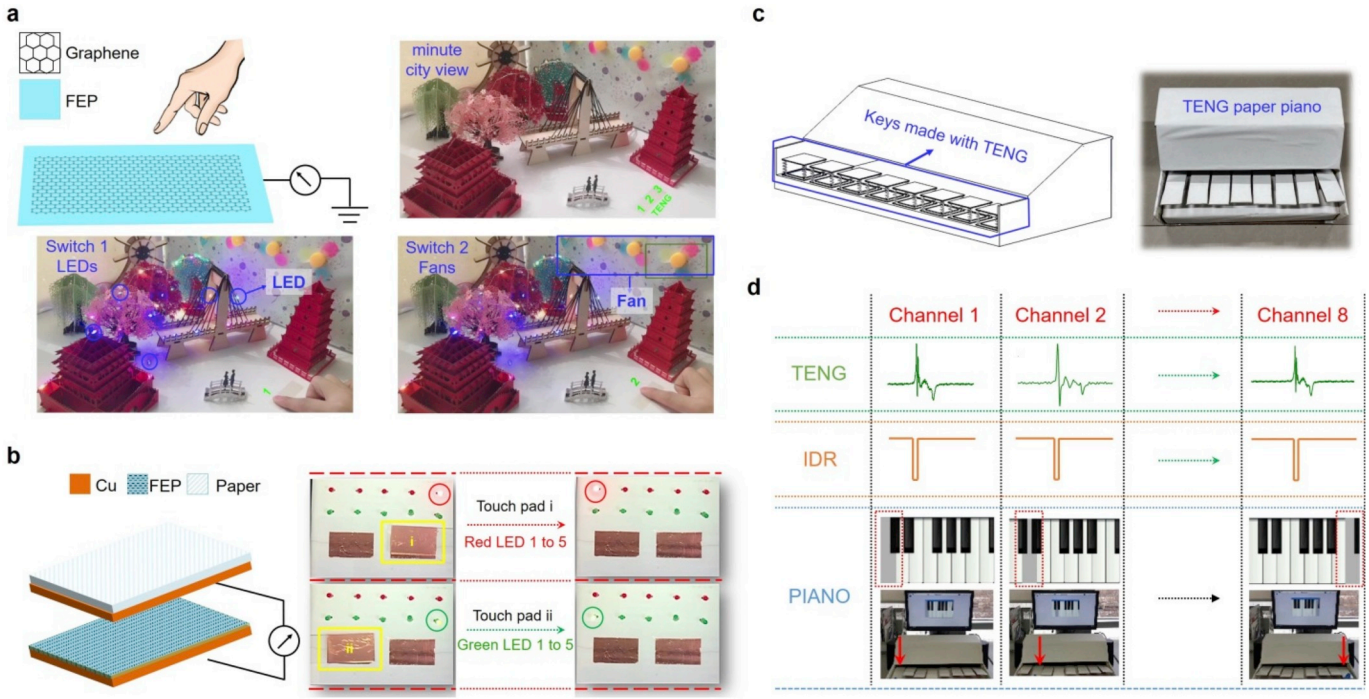

Fig. 4. Basic touch interactive applications of TIS on different substrates. (a) Schematic illustration of the graphene touch switch and the demonstrated applications in the scenes of custom minute city. (b) Paper-based contact-separation mode TENG and its application in flowing LEDs. (c) Schematic illustration and photo image of the interactive paper piano. (d) The originally irregular and messy current signals can be converted into the standard digital signals through the self-powered OC and directly read by the MCU.

We demonstrate the wireless TIS in two different scenes. The first is a ring-shaped TENG mechanosensor to control the sliding of Office Powerpoint (PPT, Microsoft Ltd.). The ring controller works in a single electrode mode, composed of the PET friction layer, ITO electrode, and textile isolation layer from skin (Fig. 5c). When the thumb touches the ring controller (*i.e.* the friction between skin and PET), the triboelectric signal is induced to trigger PPT sliding programs. Different ring controllers can also be worn on the index finger, middle finger and ring finger to achieve the functions of the sliding forward, backwards or ending (Fig. 5d). Complete processes can be viewed in Video S7. The demonstrated TIS built-in the ring controller is possible to be commercialized for the users to pay more attention on the speech and improve the presentation quality. Various embedded software programs are promising to be applicable with the ring controller.

Supplementary video related to this article can be found at https://doi.org/10.1016/j.nanoen.2019.104419.

The second demonstration of the wireless TIS is based on the textiles composed of Nylon and cotton pads with embroidered conductive Ag

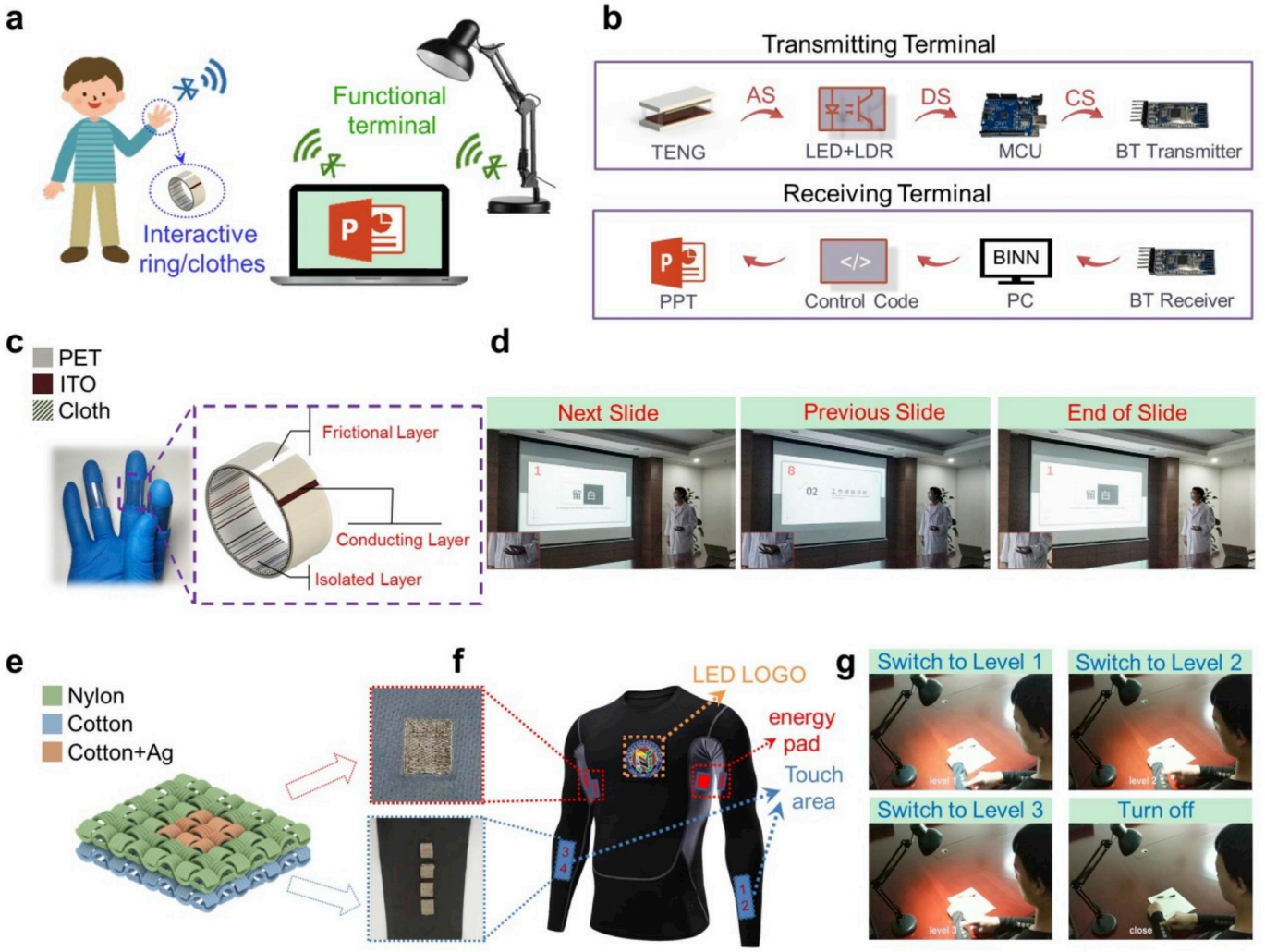

Fig. 5. (a) The concept of the wearable TIS for wireless control applications. (b) The basic working process of the wireless TIS. (c) Structural design of the ring-shaped TENG mechanosensor. (d) Demonstration of the ring-shaped TENG mechanosensor applied to control PPT. (e, f) Structural design of the textiles-based TENG and preferred positions on the clothes. (g) Demonstration of the wireless TIS based on the textiles to control desk lamp.

threads (single electrode mode, Fig. 5e). The textile based wearable TIS is facile to be embroidered on the desired position with various pattern designs (*e.g.* front, on or beneath the sleeves, Fig. 5f). When the finger touches the embroidered nylon pad, it will be positive charged according to the triboelectric sequence. Relevant triboelectric signals can be captured from different embroidered positions to control the on/off state and brightness of the desk lamp, respectively (Fig. 5g and Video S8). The photo image of the MCU, Bluetooth transmitter/receiver, circuit connections and corresponding electric signals are shown in Fig. S5. All the above demonstrations prove the versatile applications of the TIS, which is a universal and arbitrary way to IoT, intelligent robots, etc.

Supplementary video related to this article can be found at https://doi.org/10.1016/j.nanoen.2019.104419.

3. Conclusion

In this work, a universal and arbitrary tactile interactive interface based on self-powered OC has been demonstrated. As a mechanical signal collector, TENG collects external mechanical commands from the user and converts them into digital signals through a LED-photoresistor optical communicator and bleeder circuit. The digital signal can be directly recognized by the microcontroller and run the embedded program for different applications. The proposed TIS solves one of the core problems of HMI system, converting the irregular/imperfect analog signals into digital signals by using optical communication (free of inductors, capacitors, voltage comparators). Based on the TIS, we have also demonstrated basic interactive applications (transparent graphene switch, flowing LEDs and paper piano) and wireless control examples (PPT and desk lamp controller). The TIS is ready to be applicable and extended to more sophisticated interactive applications in assistance of the coming era of 5G and industry 4.0.

4. Experiments

4.1. Fabrication of the TENGs

TENG in contact-separation mode in Fig. 2a: A commercial acrylic sheet (3 mm thickness) was cut into a size of 5 × 5 cm^2 and used as the substrate for the TENG. Commercial available Cu foil and FEP film in the same size were used as the positive friction layer and negative friction layer, respectively. Another Cu foil was used as the electrodes. Graphene-based single-electrode mode TENG in Fig. 4a: The graphene grown on Cu foil (25 μm, Sigma-Aldrich) by chemical vapor deposition was firstly spin-coated with polymethyl methacrylate (PMMA) and the copper foil was etched away by soaking in etching reagent (ammonium persulfate, APS). When the copper is completely etched away, the graphene coated with PMMA was washed with deionized water for three times to remove the APS and Cu^{2+} residue, and then transferred to the

PET substrate by standard wet transfer method. Paper piano in Fig. 4c: The main body and keys of the piano were made of corrugated paper. The size of each key was 3×10 cm^2, and the effective friction size was 2×5 cm^2. Ring-shaped TENG in Fig. 5c: The as-fabricated ring-shaped TENG was approximately 2 cm in diameter and 1 cm in the ring width. The inner lining of the ring was cotton, and the outer material was commercial PET conductive film with ITO electrodes. Textiles-based single-electrode mode TENG in Fig. 5e: The conductive Ag threads were sewed on cotton pads (2×2 cm^2) by the embroidery method. Then the conductive pads are sewed on the Nylon T-shirt.

4.2. Characterization and measurements

The V_{OC} and I_{SC} of different kinds of TENGs were all measured by Keithley electrometer (6514A, Tektronix Inc., Beaverton, OR, USA). The electrical performance of photoresistors was measured by a semiconductor characterization system (Agilent 1500A).

Declaration of competing interest

The authors declare that they have no known competing financial interests or personal relationships that could have appeared to influence the work reported in this paper.

Acknowledgement

This work is financially supported by the National Key Research and Development Program of China (2016YFA0202703, 2016YFA0202704), the National Natural Science Foundation of China (51605034, 51711540300), the “Hundred Talents Program” of the Chinese Academy of Science, Beijing Nova Program (Z191100001119047) and State key laboratory of precision measuring technology and instruments (Tianjin University).

Appendix A. Supplementary data

Supplementary data to this article can be found online at https://doi.org/10.1016/j.nanoen.2019.104419.

References

[1] D. Karnaushenko, D. Makarov, M. Stöber, D.D. Karnaushenko, S. Baunack, O. G. Schmidt, High-performance magnetic sensorics for printable and flexible electronics, Adv. Mater. 27 (2015) 880–885.
[2] M. Melzer, J.I. Mönch, D. Makarov, Y. Zabila, G.S. Cañón Bermúdez, D. Karnaushenko, S. Baunack, F. Bahr, C. Yan, M. Kaltenbrunner, O.G. Schmidt, Wearable magnetic field sensors for flexible electronics, Adv. Mater. 27 (2015) 1274–1280.
[3] Y. Chen, G. Gao, J. Zhao, H. Zhang, J. Yu, X. Yang, Q. Zhang, W. Zhang, S. Xu, J. Sun, Piezotronic graphene artificial sensory synapse, Adv. Funct. Mater. 29 (2019) 1900959.
[4] X. Pu, H. Guo, J. Chen, X. Wang, Y. Xi, C. Hu, Z.L. Wang, Eye motion triggered self-powered mechnosensational communication system using triboelectric nanogenerator, Sci. Adv. 3 (2017), e1700694.
[5] Q. Sun, D.H. Ho, Y. Choi, C. Pan, D.H. Kim, Z.L. Wang, J.H. Cho, Piezopotential-programmed multilevel nonvolatile memory as triggered by mechanical stimuli, ACS Nano 10 (2016) 11037–11043.
[6] Y. Chen, J. Sun, W.J. Qiu, X.W. Wang, W.R. Liu, Y.L. Huang, G.Z. Dai, J.L. Yang, Y. L. Gao, Deep-ultraviolet SnO2 nanowire phototransistors with an ultrahigh responsivity, Appl. Phys. Mater. Sci. Process 125 (2019) 7.
[7] J. Yang, J. Chen, Y. Yang, H. Zhang, W. Yang, P. Bai, Y. Su, Z.L. Wang, Broadband vibrational energy harvesting based on a triboelectric nanogenerator, Adv. Energy Mater. 4 (2014).
[8] Q. Wang, X. Ren, S. Sarcar, X. Sun, EV-Pen: leveraging electrovibration haptic feedback in pen interaction, in: Proc. 2016 ACM Interact. Surfaces Spaces, ACM, 2016.
[9] Y. Cho, A. Bianchi, N. Marquardt, N. Bianchi-Berthouze, RealPen: Providing realism in handwriting tasks on touch surfaces using auditory-tactile feedback, in: Proc. 29th Annu. Symp. User Interface Softw. Technol. - UIST'16, 2016.
[10] C. Qian, J. Sun, L. Zhang, H.P. Xie, H. Huang, J.L. Yang, Y.L. Gao, Air-stable and high-performance organic field-effect transistors based on ordered, large-domain phthalocyanine copper thin film, Synth. Met. 210 (2015) 336–341.
[11] W. Alquraishi, Y. Fu, W. Qiu, J. Wang, Y. Chen, L.-A. Kong, J. Sun, Y. Gao, Hybrid optoelectronic synaptic functionality realized with ion gel-modulated In2O3 phototransistors, Org. Electron. 71 (2019) 72–78.
[12] J. Wang, Y. Chen, L.-A. Kong, Y. Fu, Y. Gao, J. Sun, Deep-ultraviolet-triggered neuromorphic functions in In-Zn-O phototransistors, Appl. Phys. Lett. 113 (2018) 151101.
[13] S. Ornes, Core concept: the Internet of Things and the explosion of interconnectivity, Proc. Natl. Acad. Sci. 113 (2016) 11059–11060.
[14] S. Kim, Y.J. Choi, H.J. Woo, Q. Sun, S. Lee, M.S. Kang, Y.J. Song, Z.L. Wang, J. H. Cho, Piezotronic graphene barristor: efficient and interactive modulation of Schottky barrier, Nano Energy 50 (2018) 598–605.
[15] Y. Meng, J. Zhao, X. Yang, C. Zhao, S. Qin, J.H. Cho, C. Zhang, Q. Sun, Z.L. Wang, Mechanosensation-active matrix based on direct-contact tribotronic planar graphene transistor array, ACS Nano 12 (2018) 9381–9389.
[16] J. Wang, M.-F. Lin, S. Park, P.S. Lee, Deformable conductors for human–machine interface, Mater. Today 21 (2018) 508–526.
[17] H. Kang, C. Zhao, J. Huang, D.H. Ho, Y.T. Megra, J.W. Suk, J. Sun, Z.L. Wang, Q. Sun, J.H. Cho, Fingerprint-Inspired conducting hierarchical wrinkles for energy-harvesting E-skin, Adv. Funct. Mater. 29 (2019) 1903580.
[18] R. Cao, X. Pu, X. Du, W. Yang, J. Wang, H. Guo, S. Zhao, Z. Yuan, C. Zhang, C. Li, Screen-printed washable electronic textiles as self-powered touch/gesture tribo-sensors for intelligent human–machine interaction, ACS Nano 12 (2018) 5190–5196.
[19] Y. Lee, S.H. Cha, Y.-W. Kim, D. Choi, J.-Y. Sun, Transparent and attachable ionic communicators based on self-cleanable triboelectric nanogenerators, Nat. Commun. 9 (2018) 1804.
[20] S. Lim, D. Son, J. Kim, Y.B. Lee, J.K. Song, S. Choi, D.J. Lee, J.H. Kim, M. Lee, T. Hyeon, Transparent and stretchable interactive human machine interface based on patterned graphene heterostructures, Adv. Funct. Mater. 25 (2015) 375–383.
[21] H. Chang, S. Kim, S. Jin, S.-W. Lee, G.-T. Yang, K.-Y. Lee, H. Yi, Ultrasensitive and highly stable resistive pressure sensors with biomaterial-incorporated interfacial layers for wearable health-monitoring and human–machine interfaces, ACS Appl. Mater. Interfaces 10 (2017) 1067–1076.
[22] J. Yang, J. Chen, Y. Su, Q. Jing, Z. Li, F. Yi, X. Wen, Z. Wang, Z.L. Wang, Eardrum-Inspired active sensors for self-powered cardiovascular system characterization and throat-attached anti-Interference voice recognition, Adv. Mater. 27 (2015) 1316–1326.
[23] J. Yang, J. Chen, Y. Liu, W. Yang, Y. Su, Z.L. Wang, Triboelectrification-based organic film nanogenerator for acoustic energy harvesting and self-powered active acoustic sensing, ACS Nano 8 (2014) 2649–2657.
[24] J. Liu, Y. Chen, M. Gruteser, Y. Wang, VibSense: sensing touches on ubiquitous surfaces through vibration, in: 2017 14th Annu. IEEE Int. Conf. Sensing, Commun. Networking, SECON 2017, 2017.
[25] C. Wu, W. Ding, R. Liu, J. Wang, A.C. Wang, J. Wang, S. Li, Y. Zi, Z.L. Wang, Keystroke dynamics enabled authentication and identification using triboelectric nanogenerator array, Mater. Today 21 (2018) 216–222.
[26] J. Ye, L. Xia, C. Wu, M. Ding, C. Jia, Q. Wang, Redox targeting-based flow batteries, J. Phys. D Appl. Phys. 52 (2019) 443001, 2019, J. Phys. D: Appl. Phys.
[27] J.Y. Ye, Y.H. Cheng, L.D. Sun, M. Ding, C. Wu, D. Yuan, X.L. Zhao, C.J. Xiang, C. K. Jia, A green SPEEK/lignin composite membrane with high ion selectivity for vanadium redox flow battery, J. Membr. Sci. 572 (2019) 110–118.
[28] M. Ding, G. Chen, W. Xu, C. Jia, H. Luo, Bio-inspired synthesis of nanomaterials and smart structures for electrochemical energy storage and conversion, Nano Mater. Sci. (2019), https://doi.org/10.1016/j.nanoms.2019.09.011.
[29] H.L. Zhang, Y. Yang, Y.J. Su, J. Chen, C.G. Hu, Z.K. Wu, Y. Liu, C.P. Wong, Y. Bando, Z.L. Wang, Triboelectric nanogenerator as self-powered active sensors for detecting liquid/gaseous water/ethanol, Nano Energy 2 (2013) 693–701.
[30] M. Ha, J. Park, Y. Lee, H. Ko, Triboelectric generators and sensors for self-powered wearable electronics, ACS Nano 9 (2015) 3421–3427.
[31] S.Y. Kuang, J. Chen, X.B. Cheng, G. Zhu, Z.L. Wang, Two-dimensional rotary triboelectric nanogenerator as a portable and wearable power source for electronics, Nano Energy 17 (2015) 10–16.
[32] Q.F. Shi, H. Wang, T. Wang, C. Lee, Self-powered liquid triboelectric microfluidic sensor for pressure sensing and finger motion monitoring applications, Nano Energy 30 (2016) 450–459.
[33] J. Wang, S.M. Li, F. Yi, Y.L. Zi, J. Lin, X.F. Wang, Y.L. Xu, Z.L. Wang, Sustainably powering wearable electronics solely by biomechanical energy, Nat. Commun. 7 (2016) 8.
[34] R. Vyas, V. Lakafosis, H. Lee, G. Shaker, L. Yang, G. Orecchini, A. Traille, M. M. Tentzeris, L. Roselli, Inkjet printed, self powered, wireless sensors for environmental, gas, and authentication-based sensing, IEEE Sens. J. 11 (2011) 3139–3152.
[35] N.S. Hudak, G.G. Amatucci, Small-scale energy harvesting through thermoelectric, vibration, and radiofrequency power conversion, J. Appl. Phys. 103 (2008) 24.
[36] Y.K. Fuh, H.C. Ho, Highly flexible self-powered sensors based on printed circuit board technology for human motion detection and gesture recognition, Nanotechnology 27 (2016) 8.
[37] L. Huang, S. Lin, Z. Xu, H. Zhou, J. Duan, B. Hu, J. Zhou, Fiber-based energy conversion devices for human-body energy harvesting, Adv. Mater. (2019), e1902034.
[38] X. Mo, H. Zhou, W. Li, Z. Xu, J. Duan, L. Huang, B. Hu, J. Zhou, Piezoelectrets for wearable energy harvesters and sensors, Nano Energy 65 (2019) 104033.
[39] Y. Yang, Z.H. Lin, T. Hou, F. Zhang, Z.L. Wang, Nanowire-composite based flexible thermoelectric nanogenerators and self-powered temperature sensors, Nano Res 5 (2012) 888–895.

[40] J.J. Kuchle, N.D. Love, Self-powered wireless thermoelectric sensors, Measurement 47 (2014) 26–32.
[41] E.A. Mondarte, V. Copa, A. Tuico, C.J. Vergara, E. Estacio, A. Salvador, A. Somintac, Al-doped ZnO and N-doped CuxO thermoelectric thin films for self-powering integrated devices, Mater. Sci. Semicond. Process. 45 (2016) 27–31.
[42] A.R.M. Siddique, S. Mahmud, B. Van Heyst, A review of the state of the science on wearable thermoelectric power generators (TEGs) and their existing challenges, Renew. Sustain. Energy Rev. 73 (2017) 730–744.
[43] Y. He, J. Sun, C. Qian, L. Kong, J. Jiang, J. Yang, H. Li, Y. Gao, Solution-processed natural gelatin was used as a gate dielectric for the fabrication of oxide field-effect transistors, Org. Electron. 38 (2016) 357–361.
[44] C. Qian, J. Sun, L. Kong, Y. Fu, Y. Chen, J. Wang, S. Wang, H. Xie, H. Huang, J. Yang, Y. Gao, Multilevel nonvolatile organic photomemory based on vanadyl-phthalocyanine/para-sexiphenyl heterojunctions, ACS Photonics 4 (2017) 2573–2579.
[45] L. Kong, J. Sun, C. Qian, Y. Fu, J. Wang, J. Yang, Y. Gao, Long-term synaptic plasticity simulated in ionic liquid/polymer hybrid electrolyte gated organic transistors, Org. Electron. 47 (2017) 126–132.
[46] C. Qian, L.-a. Kong, J. Yang, Y. Gao, J. Sun, Multi-gate organic neuron transistors for spatiotemporal information processing, Appl. Phys. Lett. 110 (2017), 083302.
[47] W. Ding, C. Wu, Y. Zi, H. Zou, J. Wang, J. Cheng, A.C. Wang, Z.L. Wang, Self-powered wireless optical transmission of mechanical agitation signals, Nano Energy 47 (2018) 566–572.
[48] F. Yuan, W. Li, S. Lin, N. Wu, S. Chen, J. Zhong, Z. Xu, X. Li, Y. Xiao, L. Huang, Output optimized electret nanogenerators for self-powered long-distance optical communication systems, Nanoscale 9 (2017) 18529–18534.
[49] F.-R. Fan, Z.-Q. Tian, Z.L. Wang, Flexible triboelectric generator, Nano Energy 1 (2012) 328–334.
[50] Z.L. Wang, On Maxwell's displacement current for energy and sensors: the origin of nanogenerators, Mater. Today 20 (2017) 74–82.
[51] J. Wang, C. Wu, Y. Dai, Z. Zhao, A. Wang, T. Zhang, Z.L. Wang, Achieving ultrahigh triboelectric charge density for efficient energy harvesting, Nat. Commun. 8 (2017) 88.
[52] Z.L. Wang, L. Lin, J. Chen, S. Niu, Y. Zi, Triboelectric Nanogenerators, Springer, 2016.
[53] R. Liu, X. Kuang, J. Deng, Y.C. Wang, A.C. Wang, W. Ding, Y.C. Lai, J. Chen, P. Wang, Z. Lin, Shape memory polymers for body motion energy harvesting and self-powered mechanosensing, Adv. Mater. 30 (2018) 1705195.
[54] G. Gao, J. Yu, X. Yang, Y. Pang, J. Zhao, C. Pan, Q. Sun, Z.L. Wang, Triboiontronic transistor of MoS2, Adv. Mater. 31 (2019) 1806905.
[55] Q. Zhang, T. Jiang, D. Ho, S. Qin, X. Yang, J.H. Cho, Q. Sun, Z.L. Wang, Transparent and self-powered multistage sensation matrix for mechanosensation application, ACS Nano 12 (2017) 254–262.
[56] Z.L. Wang, Triboelectric nanogenerators as new energy technology for self-powered systems and as active mechanical and chemical sensors, ACS Nano 7 (2013) 9533–9557.
[57] Q. Shi, C. Lee, Self-powered bio-inspired spider-net-coding interface using single-electrode triboelectric nanogenerator, Adv. Sci. 6 (2019) 1900617.
[58] Q. Shi, Z. Zhang, T. Chen, C. Lee, Minimalist and multi-functional human machine interface (HMI) using a flexible wearable triboelectric patch, Nano Energy 62 (2019) 355–366.
[59] X.P. Hengyu Guo, Jie Chen, Yan Meng, Min-Hsin Yeh, Guanlin Liu, Qian Tang, Baodong Chen, Di Liu, Song Qi, Changsheng Wu, Chenguo Hu, Jie Wang, Zhong Lin Wang, A highly sensitive, self-powered triboelectric auditory sensor for social robotics and hearing aids, Sci. Robot. 3 (2018) eaat2516.
[60] D.-W. Shin, M.D. Barnes, K. Walsh, D. Dimov, P. Tian, A.I.S. Neves, C.D. Wright, S. M. Yu, J.-B. Yoo, S. Russo, M.F. Craciun, A new facile route to flexible and semi-transparent electrodes based on water exfoliated graphene and their single-electrode triboelectric nanogenerator, Adv. Mater. 30 (2018) 1802953.